Comparative Study of the Metal Organic Chemical Vapor Deposition of β-CoGa Thin Films from Dialkylgallium Tetracarbonylcobaltate Single-Source Precursors

Roland A. Fischer* and Alexander Miehr

Anorganisch-chemisches Institut, Technische Universität München, Lichtenbergstrasse 4, D-85747 Garching, Germany

Received August 21, 1995. Revised Manuscript Received November 17, 1995[⊗]

The volatile heterodinuclear organometallic compounds $L(CO)_3Co-GaR_2(Do)$ and $L(CO)_3Co-Ga[(CH_2)_3NR^1_2](R)$ (R = H, CH_3, C_2H_5, $CH_2{}^tBu$, CH_2SiMe_3; Do = THF, NMe_3, NC_7H_{13}; L = CO, PMe_3, PPh_3; $R^1 = CH_3$; C_2H_5; **1**−**10** were studied as single molecule precursors for the deposition of binary Co/Ga alloy thin films by MOCVD using a horizontal hot-walled reactor in the absence of carrier gases in vacuo. The metal concentrations of the thin films were found to depend on the substrate temperature and the type of substituents at the gallium atom. Cobalt-rich films were typically deposited below 250 °C. The 1:1 ratio of the metals in the precursor compounds is retained above 300−350 °C. Typical growth rates were between 0.1 and 1 μm h^{-1} at ∼1 Pa total pressure. The best results were obtained with the precursor compound $(CO)_4Co-GaEt_2(NMe_3)$ (**5a**). The grown films showed impurity levels of C, N, and O close to the detection limit of the used analytical methods (≤0.5 at. % by AES). The thin-film resistivities were around 150(±30) μΩ cm in these cases. At substrate temperatures below 300 °C, alkyl-transfer reactions are important, which are likely to be surface driven. These processes generate volatile and thermally stable gallium alkyls GaR_3, which pass through the reaction zone. This mechanism explains the gallium deficiency of the Co_1Ga_{1-x} films grown at low substrate temperatures. Other byproducts were mainly unsaturated hydrocarbons (e.g., ethene or $H_2C{=}CHCH_2NMe_2$) and nonfragmented donor ligands Do (e.g., THF, NMe_3). The films were routinely examined ex situ by SEM-EDX and AUGER electron spectroscopy. Films grown on various substrates (quartz, GaAs, silicon) were structurally characterized by X-ray diffraction showing the cubic β-CoGa as the only detectable crystalline phase in the case of GaAs(100) and quartz substrates (ca. 300 °C substrate temperature). At higher deposition temperatures (350−380 °C for GaAs and 400−450 °C for silicon) interfacial solid-state reactions occurred to give various other phases such as α-$Co_{1-\delta}Ga_\delta$, β-CoGa, $CoGa_3$, CoAs, and Co_2Si.

Introduction

The intermetallic phase β-CoGa has been identified as an epitaxial and thermodynamically stable metal GaAs semiconductor interface, which can serve as a novel tunable Schottky barrier.[1,2] Kaesz et al. have recently demonstrated the epitaxial growth of β-CoGa on GaAs(100) from two independent sources, $(\eta^5-C_5H_5)(CO)_2Co$ and an excess of $Ga(C_2H_5)_3$, at atmospheric pressure in the presence of hydrogen (cold-wall reactor).[3] The deposition of polycrystalline β-CoGa from the known compound $(CO)_4Co-GaCl_2(THF)$ (**1**)[4] has also been reported by the same authors (isothermal hot-wall reactor).[5−7] Aiming at alternative "single-source precursors" for β-CoGa, which are more volatile than **1**, free of halide substituents, and which may decompose more cleanly even under vacuum conditions in the absence of additional carrier gases,[8] we have been investigating the chemistry of alkyl derivatives of **1** during the past years.[9−11] In this work we now describe our studies on the deposition of β-CoGa thin films from those novel precursors of the general formulas $L(CO)_3Co-GaR_2(Do)$ and $L(CO)_3Co-Ga[(CH_2)_3NR^1_2](R)$ (R = H, CH_3, C_2H_5, $CH_2{}^tBu$, CH_2SiMe_3; Do = THF, NMe_3, NC_7H_{13}; L = CO, PMe_3; $R^1 = CH_3$; C_2H_5; **2**−**10**; see Figure 1 and Table 1).

Experimental Section

Precursor Preparation, Characterization and Handling. All manipulations were carried out under dry and oxygen-free nitrogen or argon atmosphere using oven-dried glassware. Solvents were freshly distilled from Na/K alloy. The synthesis of $L(CO)_3Co-GaR_2(Do)$ and $L(CO)_3Co-Ga[(CH_2)_3NR^1_2](R)$ (R = Cl, H, CH_3, C_2H_5, $CH_2{}^tBu$, CH_2SiMe_3; Do = THF, NMe_3, NC_7H_{13}; L = CO, PMe_3, PPh_3; $R^1 = CH_3$; C_2H_5; **1**−**10**) from $[L(CO)_3Co](K)$ and $ClGaR_2(Do)$ or $ClGa[(CH_2)_3NR^1_2](R)$ on a typical scale of 10−20 mmol (5−10 g) has

* To whom correspondence should be addressed at Anorganisch-chemisches Institut, Ruprecht-Karls Universität Heidelberg, Im Neuenheimer Feld 270, D-69120 Heidelberg, Germany.

⊗ Abstract published in *Advance ACS Abstracts,* January 1, 1996.

(1) Williams, R. S. *Appl. Surf. Sci.* **1992**, *60/61*, 613.
(2) Kuo, T. C.; Wang, K. L.; Arghavani, R.; George, T.; Lin, T. L. *J. Vac. Sci. Technol.* **1992**, *B10*, 1923.
(3) Maury, F.; Talin, A. A.; Kaesz, H. D.; Williams, R. S. *Chem. Mater.* **1993**, *5*, 84.
(4) Patmore, D. J.; Graham, W. A. G. *Inorg. Chem.* **1966**, *5*, 1586.
(5) Kaesz, H. D.; Williams, R. S.; Hicks, R. F.; Zink, J. I.; Chen, Y.-J.; Müller, H.-J.; Xue, Z.; Xu, D.; Shuh, D. K.; Kim, Y. Y. *New J. Chem.* **1990**, *14*, 527.
(6) Chen, Y.; Kaesz, H. D.; Kim, Y. K.; Müller, H. J.; Williams, R. S.; Xue, Z. *Appl. Phys. Lett.* **1989**, *55*, 2760.
(7) Maury, F.; Brandt, L.; Kaesz, H. D. *J. Organomet. Chem.* **1993**, *449*, 159.
(8) Zinn, A. ;. N., B.; Kaesz, H. D. *Adv. Mater.* **1992**, *4*, 375.
(9) Fischer, R. A.; Miehr, A.; Priermeier, T. *Chem. Ber.*, in press.
(10) Fischer, R. A.; Behm, J. *Chem. Ber.* **1992**, *125*, 37.
(11) Fischer, R. A.; Behm, J. *J. Organomet. Chem.* **1992**, *429*, 275.

0897-4756/96/2808-0497$12.00/0

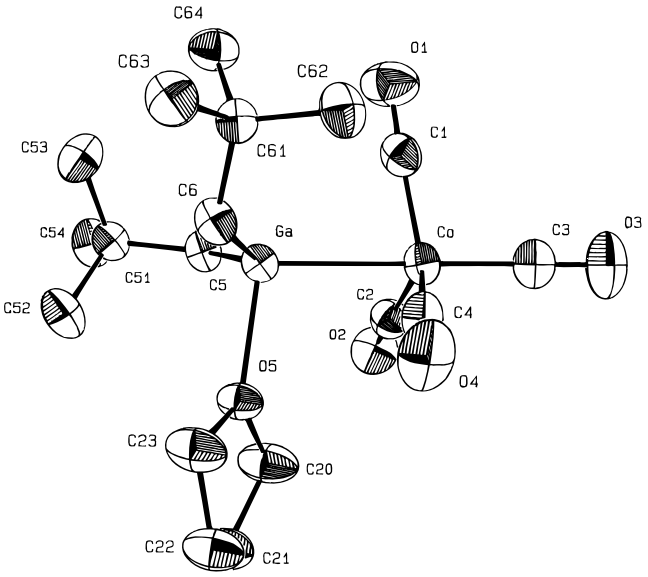

Figure 1. Molecular structure of $(CO)_4Co-Ga(CH_2{}^tBu)_2(C_4H_8O)$ (**6a**) as the prototype of the compound series $L(CO)_3Co-GaR_2(Do)$ (**1**−**6**), obtained from a single-crystal X-ray diffraction study (ORTEP drawing; the thermal ellipsoids are drawn at a 50% level; hydrogen atoms are omitted for clarity). For schematic drawings of the precursors **7**−**10**, see Scheme 1.

Table 1. Numbering Scheme of the Precursor Compounds

Precursor Type $L(CO)_3Co-GaR_2(Do)$

compound no.	R	Do	L
1	Cl	THF	CO
2	Cl	NMe_3	PMe_3
3	H	NMe_3	CO
4a	Me	THF	CO
4b	Me	NMe_3	CO
5a	Et	NMe_3	CO
5b	Et	NC_7H_{13}	CO
6a	CH_2CMe_3	THF	CO
6b	CH_2SiMe_3	THF	CO

Precursor Type $L(CO)_3Co-Ga[(CH_2)_3NR^1_2](R)$

compound no.	R	R^1	L
7a	Et	Me	CO
7b	Et	Me	PMe_3
8a	^{t}Bu	Et	CO
8b	^{t}Bu	Me	CO
9	Me	Et	PPh_3

Precursor Type $[L(CO)_3Co]_2Ga[(CH_2)_3NR^1_2]$

compound no.	R^1	L
10	Et	CO

been described in detail elsewhere (Scheme 1, Table 1).[9−11] The compounds (except **3** and **9**) sublime quantitatively without decomposition at 25−90 °C and 0.1−10 Pa with practical rates up to 2−3 g h^{-1}. Simple experiments to check the vapor pressure (tensiometric with a Baratron gauge) gave values of 0.1−0.5 Pa at 25 °C and values of 1−5 Pa at 80−90 °C. All manipulations with the precursor compounds should be conducted by a skilled person using inert-gas techniques and a closed apparatus (e.g., Schlenk-line or glovebox) in combination with a good ventilated hood. Due to the significant volatility of the compounds and their partial hydrolysis into volatile $[L(CO)_3Co-H]$ and $\{[\mu^2-(HO)]GaR_2\}_3$ in air[10] (both these compounds may exhibit a significant toxicity), care must be taken to avoid inhalation. The compounds are not pyrophoric and can be stored under inert-gas atmosphere with cooling (−10 °C) for an unlimited period of time. However, some of compounds (**5a**) are extremely moisture sensitive, and the use of passivated glassware (boiling out with Me_2SiCl_2) is recommended, if very pure conditions are required. Any residues of the precursors can be destroyed safely either by careful oxidative acid hydrolysis with dilute H_2O_2/H_2SO_4 (with cooling to 0 °C) or by dissolution into 2-propanol/KOH.

Scheme 1. Synthesis of the Complexes of Type 1−10[a]

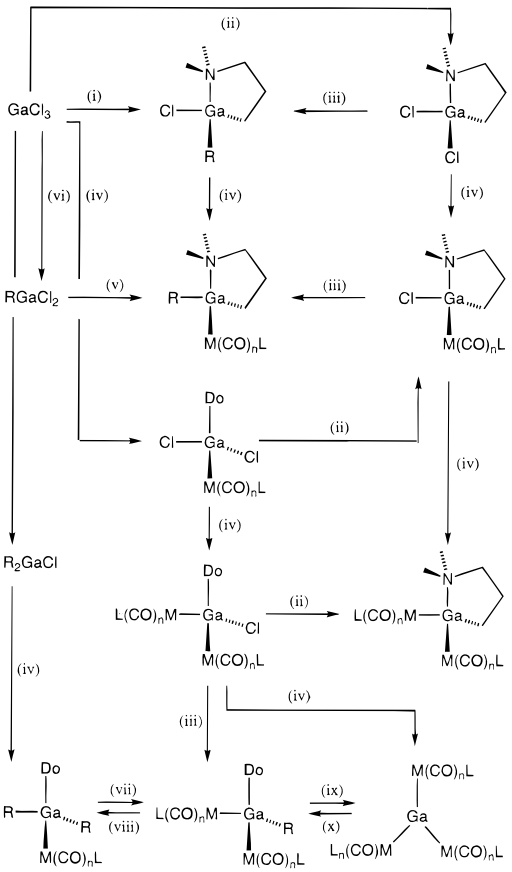

[a] (i) 1, R_4Si; 2, $Li[(CH_2)_3NMe_2]$, Et_2O. (ii) $Li[(CH_2)_3NMe_2]$, Et_2O, 25 °C. (iii) R = alkyl, aryl: RLi, toluene; R = H: $Li[BEt_3H]$, THF; $R = BH_4$: $Li[BH_4]$, Et_2O. (iv) $[L(CO)_nM](Na/K)$; L = CO: toluene, pentane; L = Cp, PR_3: THF, Et_2O. (v) R = H, alkyl: 1, $Li[(CH_2)_3NMe_2]$, pentane; 2, $[L(CO)_nM](Na/K)$. (vi) Me_3SiH; (vii) − $DoGaR_3$; (viii): + $DoGaR_3$; (ix): − $DoGa[M]R_2$; (x) + $DoGa[M]R_2$, + Do ([M] = $[L(CO)_nM]$). For details see ref 9.

NMR spectra were recorded using a JEOL GMX 400 spectrometer (C_6D_6, 20 °C). Elemental analysis were obtained from the Microanalytic Laboratory of the Technical University Munich. Mass spectra were recorded on Finnigan MAT 90 (EI, 70 eV) and Varian MAT 311a (FI and CI with isobutene) spectrometers. Gas chromatographic analyses were performed using a HP 5890 equipped with a mass selective detector system (HP 5970B). A fused silica capillary column (HP-1, #19091Z-102 with 100% methylpolysiloxane (l = 50 m, i.d. = 0.2 mm, film thickness 0.33 μm) was used. The molar fractions of the observed gaseous constituents are reported on the bases of noncalibrated total ion currents.

Film Deposition by MOCVD. The vacuum MOCVD experiments were carried out in an isothermal horizontal hot-walled quartz tube reactor described in detail elsewhere.[12] The substrates for CVD studies consisted of borosilicate microscope slides, quartz, silicon(111) slides, and GaAs(100) slides, which were cleaned by degreasing in trichloroethylene, 2-propanol/acetone, rinsing with deionized water and treating by usual etching procedures. After the reactor was charged with various substrates, the system was evacuated to a base pressure of $<10^{-4}$ Pa (turbo molecular pump, Edwards EXT 250) and heated to 350 °C for several hours. The precursor

(1) Fischer, R. A.; Kleine, M.; Lehmann, O.; Stuke, M. *Chem. Mater.* **1995**, *7*, 1863.

reservoir was loaded under an inert gas atmosphere with 1−2 g of the precursor compound and cooled to −30 °C. Then the valve to the reactor was opened and the system was evacuated again to 10^{-4} Pa for several hours. The temperature of the furnace was set at the desired value and was allowed to stabilize. The temperature profile of the furnace (i.d. = 40 mm; l = 40 cm) was measured showing a maximum negative deviation of 30 °C from the temperature at the center (200−400 °C). The temperature of the precursor reservoir was then adjusted to 35−80 °C allowing the precursors to sublime through the hot zone at pressures of 0.1−10 Pa. Reflective metallic depositions formed on the wall of the tube and on the substrates. Carrier gases were not used in these experiments.

Thin-Film Characterization. The films obtained were examined ex situ by various surface analytic tools (AES and SEM-EDX) and X-ray powder diffraction. The metal ratio was determined independently by AAS after quantitative dissolution of representative films in aqueous nitric acid (p.a.; 6.5 wt %). Thick films were grown on the walls of the reaction tube, which peeled off by rapid cooling of the tube (10 °C s^{-1}). After collecting typical quantities of 50−100 mg of the deposited material, classical combustion analysis was performed (C, H, and N). The compositions of the films were uniform over the plated areas of typically ∼3 cm^2 (AES mapping and profiling). The EDX spectra were recorded using a scanning electron microscope JEOL JSM-35C equipped with an EG&G Ortec System 5000 X-ray analysator system. A typical standardless program for quantitative analysis AUTOZAP 3.08 (ZAF correction) was employed. The obtained values for the Co and Ga contents were found to be valid within a relative error of ±20% (comparison with AAS values and a $Co_{0.50}Ga_{0.50}$ standard prepared by classical metallurgical procedures). AUGER electron spectra were recorded using a PHI 595 spectrometer with a base pressure of (2−4) × 10^{-7} Pa and a working pressure of (2−5) × 10^{-6} Pa with a standard cylindrical mirror analyzer (3 keV primary beam energy, 0.2 μA primary beam intensity, a maximum of 500 Å lateral resolution; rate of argon ion sputtering 300 Å s^{-1} on Ta_2O_5 for an area of 1 × 1 mm). Typical data collection time was 30 min for 1 keV scan width. The films were cleaned first by 5 min of argon ion (Ar^+, 3 keV) sputtering (5 × 5 mm area) at a pressure of 5 × 10^{-4} Pa. The quantitative analysis of the obtained spectra was based on differentiated spectra and accepted standard sensitivity factors[13−15] for C (0.18), N (0.32), O (0.50), Co (0.27), and Ga (0.13). The results agree with the AAS and EDX values. The specific resistivity of the deposited metallic coatings were routinely checked by a usual commercial four point probe system (FPP-5000, Veeco). The analytical data are compiled in Table 2.

Structural Characterization. The X-ray diffraction patterns were recorded on a Huber-Guinier diffractometer 653; Ge-monochromated Cu Kα (λ = 1.540 56 Å) using the step scanning method with an angle of incidence of 3°, a scan width of 0.005° (counting time of 10 s) and a rotating probe head. The measured θ values were calibrated against polycrystalline Si powder. The results of typical measurements of a β-CoGa films deposited from **8a** on silica and from **5a** on GaAs(100) at 300 °C and 0.1 Pa are compiled in Table 3 and Figure 6. β-CoGa, P_{m3m} (Int. Tab. 221), a = 287.8(3) pm, V = 23.86 × 10^6 pm^3, ρ_{calc} = 8.9 g cm^{-3}.

Byproduct Analysis. The exhaust gases of the vacuum MOCVD experiments were monitored in situ by a quadrupolar mass spectrometer (gas analysis system HPR30-HAL/3F, 1−510 amu; HIDEN) which was connected to the apparatus by a gas sampling unit with a pinhole (i.d. = 0.7 mm). The condensables were collected in a cold trap attached to the reactor chamber. After the deposition experiment was completed, the cold trap was isolated from the remaining apparatus and the contents were vacuum-transferred into a NMR tube. C_6D_6 was added and the NMR tube was sealed. The tube contents were analyzed by ^{1}H NMR and ^{13}C NMR spectroscopy. Subsequently the NMR tube was opened again and the contents were characterized by a GC-MS analysis system. The results of a typical experiment with **5a** as precursor (#31 of Table 2c) are as follows. The predominant species (Σ > 99 mol %; GC/MS) of the collected condensable effluent were identified as C_2H_4 (62%), C_2H_6 (6%), and $N(CH_3)_3$ (31%). When the precursor compound **8a** was used, the typical pattern of the organic fragments of the effluent was dominated by $Me_2C{=}CH_2$, $H_2C{=}CHCH_2NEt_2$, *cis*/*trans*-$CH_3CH{=}CHNEt_2$, and $CH_3CH_2CH_2NEt_2$. The ratio of unsaturated-to-saturated amines was calculated to 4:1. In the case of typical low-temperature vacuum MOCVD experiments, e.g., nos. 1, 2, 6, and 29 of Table 2, the condensables were fractionally distilled from the cold trap at 0 °C in vacuo. Using this procedure, an oily colorless and less volatile residue remained. This residue was vacuum transferred into a small Schlenk tube at 50 °C and 0.1 Pa and was identified as GaR_3 or $R_2Ga[(CH_2)_3NR^1_2]$ and some traces of $RGa[(CH_2)_3NR^1_2]_2$ by mass spectroscopy and NMR. The metal content of the condensables was measured in various experiments after aqueous work up (hydrolysis with HNO_3, 6.5 wt %) using AAS showing typical values of n(Co)/n(Ga) ≤ 10^{-2} for substrate temperatures between 200 and 250 °C. Table 4 contains a representative mass balance with respect to the metals Co and Ga, which was performed using precursor **5a**, a reactor temperature of 350 °C, and a pressure of 10 Pa (the precursor reservoir was set at 45 °C).

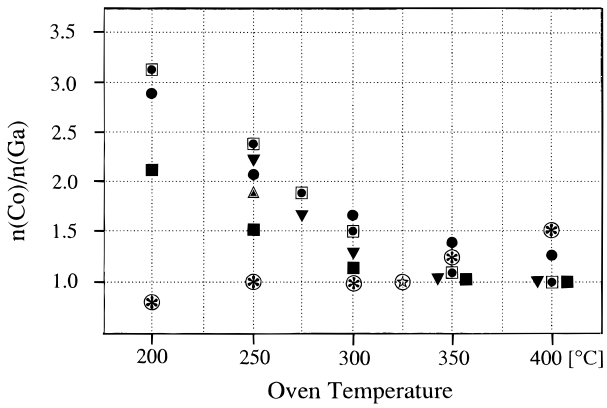

Figure 2. Temperature dependence of the ratio n(Co)/n(Ga) of the thin CoGa films obtained from different precursors at p = 1−2 Pa. Symbols: ■ = $(CO)_4CoGaEt_2(NMe_3)$ (**5a**), exp. no. 29−32; ⊡ = $(CO)_4CoGa[(CH_2)_3NEt_2]({}^t\text{Bu})$ (**8a**), exp. no. 2−3, 5, 12, 16−17; ▼ = $(CO)_4CoGa[(CH_2)_3NMe_2](Et)$ (**7a**), exp. no. 4, 6−7, 10−11, 13; ● = $(CO)_4CoGa(CH_2{}^t\text{Bu})_2(THF)$, exp. no. 1, 8, 24; ∗ = $(CO)_4CoGaCl_2(THF)$ (**1**), atmospheric pressure CVD, flow system with N_2/H_2, data taken from ref 7; ☆ $(Me_3P)(CO)_3CoGaCl_2(NMe_3)$ (**2**), exp. no. 36 (not included in Tables 2-c); ▵ $(Me_3P)(CO)_3CoGa[(CH_2)_3NMe_2](Et)$ (**7b**), exp. no. 34 (not included in Table 2c).

Results and Discussion

A series of thermal MOCVD experiments was conducted with the precursors **1**−**8** and **10** (**9** is not volatile) using a horizontal hot-walled vacuum CVD reactor *without* carrier gases under nearly isothermal conditions. A selection of typical results of the thin film analysis are summarized in Tables 2−4.

A. Metal Ratio of the Thin Films and Control of Composition. Results. Figure 2 shows the dependence of the metal ratio n(Co)/n(Ga) of the films as a function of the substrate temperature for a series of selected precursors. Within the investigated temperature range of 200−400 °C, the precursors **4**−**8** gave very

(13) Davis, L. E.; McDonald, N. C.; Palmberg, P. W.; Riach, G. E.; Weber, R. E. *Handbook of Auger Elektron Spectroscopy*, 2nd ed.; Physical Electronics Inc.: Eden Prairie, MN, 1976.
(14) Sekine, T.; Nagasawa, M. K.; Sakai, Y.; Parkes, A. S.; Geller, J. D.; Mogami, A.; Hirata, K. *Handbook of AUGER Electron Spectroscopy*; JEOL: Tokyo, 1982.
(15) McGuire, G. E. *Auger Electron Spectroscopy Reference Manual*; Plenum Press: New York, 1979.

Table 2

(a) Selected Analytical Data of Thin CoGa Films Grown from Precursor **7a** (Borosilicate Glass Substrates)

precursor	$(CO)_4Co-Ga[(CH_2)_3NMe_2](Et)$ (**7a**)					
T [°C] (±5)	200	250	285	300	350	400
expt no.	6	7	11	4	10	13
Co [μg] (±10)	334	484	570	429	1136	276
Ga [μg] (±10)	123	242	357	347	1235	319
pressure [Pa]	∼1	∼1	∼1	∼1	∼1	∼1
coated area [cm^2]	3.2	3.2	3.2	3.2	3.2	3.2
deposition time [h]	2	2	2	2	4	1
growth rate [μm/h]	0.08	0.13	0.16	0.14	0.20	0.21
n(Co)/*n*(Ga)	3.2	2.4	1.9	1.5	1.1	1.0
Co_1Ga_{1-x}:*x*	0.69	0.58	0.47	0.33	0.07	0.02
Co [at. %] (±2)	65[a]	47	53[a]	60	47	46
Ga [at. %] (±2)	20[a]	20	28[a]	40	43	44
C [at. %] (±2)	15[a]	16	13[a]		6	5
H [at. %] (±2)		17			5	4
C/H		0.9			1.2	1.3
O [at. %] (±1)	≪1[a]		5[a]		2	3
N [at. %] (±1)	≪1[a]		≪1[a]			

(b) Selected Analytical Data of Thin CoGa Films Grown from Precursor **8a** (Borosilicate Glass Substrates)

precursor	$(CO)_4Co-Ga[(CH_2)_3NEt_2]({}^tBu)$ (**8a**)					
T [°C]	250	250	285	300	350	400
expt no.	2	5	3	16	12	17
Co [mg] (±10)	172	118	550	1491	445	1029
Ga [mg] (±10)	97	69	397	1345	478	1111
pressure [Pa]	∼0.1	∼0.1	∼1	∼10	∼1	∼1
coated area [cm^2]	3.2	3.2	3.2	3.2	3.2	3.2
deposition time [h]	4	4	2	2	2	4
growth rate [μm/h]	0.02	0.02	0.17	0.50	0.16	0.19
n(Co)/*n*(Ga)	2.1	2.1	1.6	1.3	1.08	1.10
Co_1Ga_{1-x}:*x*	0.52	0.52	0.38	0.23	0.07	0.09
Co [%] (±2)	53[a]	44			47[a]	43
Ga [%] (±2)	27[a]	21			46[a]	39
C [%] (±2)	15[a]	16			4[a]	9
H [%] (±2)		19				8
C/H		0.86				1.1
O [%] (±1)	≪1[a]	≪1[a]			3[a]	3
N [%] (±1)	≪1[a]	≪1[a]			≪1[a]	≪1[a]

(c) Selected Analytical Data of Thin CoGa Films Grown from the Precursors **5a** and **6a**

precursor	$(CO)_4Co-GaNp_2(THF)$ (**6a**)			$(CO)_4Co-GaEt_2(NMe_3)$ (**5a**)		
T [°C]	200	300	400	200	300	400
expt no.	1	8	24	29	31	32
Co [mg] (±10)	401	477	519	271	580	674
Ga [mg] (±10)	171	350	506	155	590	785
pressure [Pa]	∼1	∼1	∼1	∼1	∼1	∼1
coated area [cm^2]	3.2	3.2	3.2	3.2	3.2	3.2
deposition time [h]	2	2	2	2	2	2
growth rate [μm/h]	0.10	0.15	0.18	0.14	0.21	0.26
n(Co)/*n*(Ga)	2.8	1.6	1.2	2.1	1.2	1.0
Co_1Ga_{1-x}:*x*	0.64	0.23	0.17	0.52	0.17	0.02
Co [%]	66	55	49	67	54	50
Ga [%]	24	35	41	32	45	49
C [%] (±2)	6[a]	4[a]	7[a]	≪1[a]	≪1[a]	≪1[a]
H [%] (±2)						
C/H						
O [%] (±1)	4[a]	6[a]	3[a]	1[a]	1[a]	1[a]
N [%] (±1)				≪1[a]	≪1[a]	≪1[a]

[a] Values obtained by AES.

uniform (SEM) metallic and reflective depositions of the general composition Co_1Ga_{1-x}. The 1:1 metal ratio of the precursor compounds is not necessarily reproduced in the thin films. Films grown in the "low-temperature range" of 200−300 °C tend to be Ga deficient, while films grown above 350 °C are usually stoichiometric. Cobalt-rich precursors, taking $[(CO)_4Co]_2Ga[(CH_2)_3NMe_2]$ (**10**) as a representative example, do not show a significant variation of the metal ratio with the substrate temperature.

In most cases (except precursor **3**), the metal distribution of the films proved to be very uniform over the plated areas and depths (no significant variation by AES mapping and depth profiling; see Figures 3 and 4). The parameter of the gallium loss, *x*, mainly depends on the substrate temperature and the type of substituents at the gallium atom, but it is much less dependent on the pressure (varied between 0.1 and 10 Pa by adjusting the temperature of the precursor reservoir) which reflects the total mass flow of the precursor. The films

Table 3. Observed X-ray Diffraction Intensities of a Typical Stoichiometric β-$Co_{0.50}Ga_{0.50}$ Thin Film Grown from $(CO)_4Co-Ga[(CH_2)_3NEt_2]({}^tBu)$ (8a) on Silica at 350 °C

hkl	rel int	*d* [Å] (exp)	2θ [deg] (calc)	2θ [deg][a]	2θ [deg] (exp)
100		2.8788	31.04		
110	100	2.0356	44.47	44.53	44.64
111		1.6620	55.22		
200	10	1.4394	64.71	64.76	64.80
210		1.2874	73.50		
211	8	1.1752	81.90	81.90	81.92
220	4	1.0178	98.36	98.40	98.50
221		0.9596	106.78		
310	7	0.9103	115.58	115.62	115.66

[a] Data taken from ref 59.

Table 4. Mass Balance for the Metal Content of the Deposition Experiment No. 31 of Table 2c (Precursor 5a, Borosilicate Glass Substrates, of 3.2(±1) cm^2 Coated Area; Calcd Growth Rate 0.2 μm/h)

expt no.	Co [mg]	Ga [mg]	*n*(Co)/*n*(Ga)	*m* [mg]	M [mmol]
precursor (beginning)	380	450	1.00	820	2.30
precursor (end)	97	108	1.05	575	
precursor (volatilized)	40.1	48.2	1.00	245	0.68
tube wall	37.4	45.0	0.98	82.4	0.64
substrate no. 1					
AAS	0.58	0.59	1.16	1.17	
AES			1.2		
substrate no. 2					
AAS	0.45	0.48	1.10	0.93	
AES			1.2		
substrate #3					
AAS	0.28	0.26	1.27	0.54	
AES			1.3		
total mass of the films	38.7	46.3	0.99	85.0	0.66
trap content	0.05	0.11	0.53		
balance found	38.8	46.4		85.2	
balance calcd				88.5	

grown from trans phosphine substituted precursors, e.g., $(Me_3P)(CO)_3Co-Ga[(CH_2)_3NMe_2](Et)$ (**7b**), do not show a significant deviation of their metal content from those films which were grown from the related trans carbonyl-substituted precursor (**7a**). Gallium-rich films, *n*(Co)/*n*(Ga) < 1, were not obtained from the precursors **4**−**8**. The unstable precursor $(CO)_4Co-GaH_2(NMe_3)$ (**3**) is an exception in this respect. In this case CoGa films with a significant variation of the metal ratio through the depth of the film were grown at rather low substrate temperatures (Figure 3a).

The analysis of the condensable effluent of the various MOCVD experiments showed the presence of alkylgallium compounds GaR_3 or $R_2Ga[(CH_2)_3NR^1_2]$[16] and some traces of $RGa[(CH_2)_3NR^1_2]$.[17] For example, using the precursor **6b** and a substrate temperature of 250 °C, $Ga(CH_2SiMe_3)_3$ was isolated from the contents of the cold trap as the only detectable Ga species. A related mass balance of a typical deposition experiment using the precursor **5a** at the "high-temperature" range is given in Table 3, showing virtually no loss of gallium as $GaEt_3$ in this case.

Discussion. During the MOCVD experiments reorganization processes of the substituents at the gallium center occur, which may lead to the formation of some

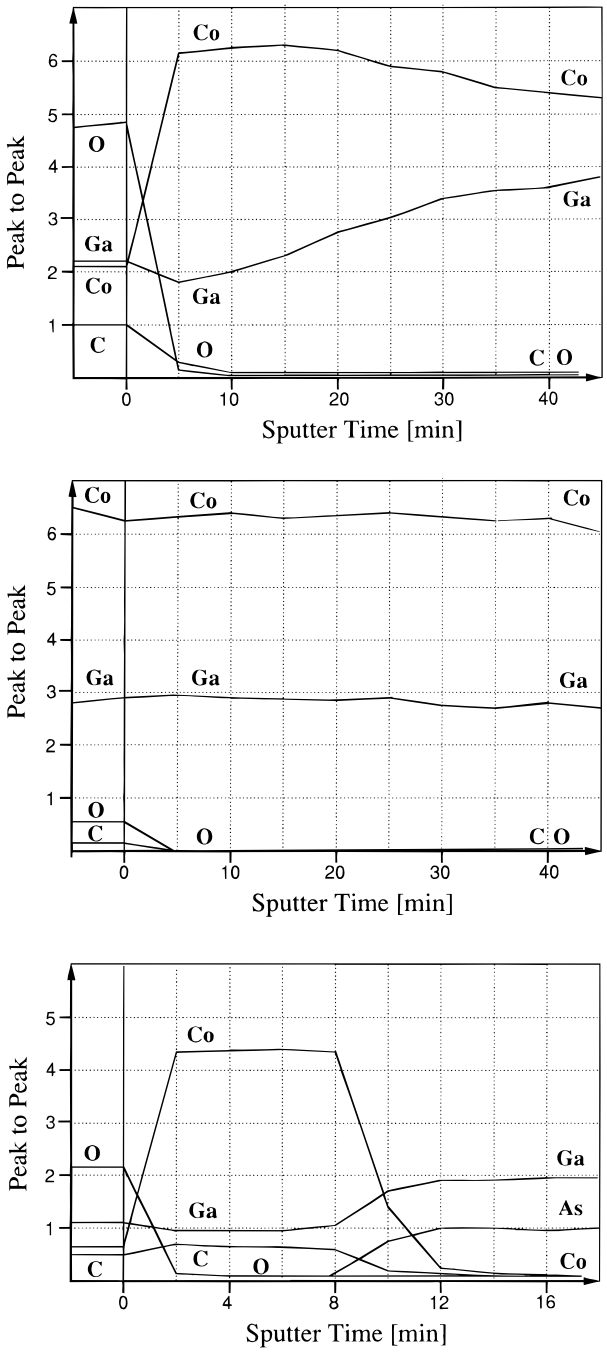

Figure 3. AES depth profiles: (a, top) CoGa film grown from $(CO)_4CoGaH_2(NMe_3)$ (**3**) (exp. no. 21, not included in Table 2c). (b, middle) CoGa film grown from $(CO)_4CoGaEt_2(NMe_3)$ (**5a**) (exp. no. 14, at 350 °C, 1 Pa, not included in Table 2c). (c, bottom) CoGa film grown from $(CO)_4CoGa[(CH_2)_3NMe_2](Et)$ (**7a**) (exp. no. 6, see Table 2a).

gallium alkyl compounds. These compounds, being relatively stable toward further pyrolysis, pass through the heated reaction zone and collect in the cold trap. This process accounts for the gallium deficiency of films grown in the low temperature range. It resembles the well known tendency of organogallium transition-metal compounds to undergo exchange equilibria in solution (Scheme 2).[18,19] For the transition-metal component cobalt, a similar mechanism to produce a rather stable

(16) Schumann, H.; Hartmann, U.; Wassermann, W.; Just, O.; Dietrich, A.; Pohl, L.; Hostalek, M.; Lokai, M. *Chem. Ber.* **1991**, *124*, 1113.

(17) Schumann, H.; Seuss, T. D.; Just, O.; Weimann, R.; Hemling, H.; Gorlitz, F. H. *J. Organomet. Chem.* **1994**, *479*, 171.

(18) Fischer, R. A.; Behm, J. *J. Organomet. Chem.* **1991**, *413*, C10.

(19) Fischer, R. A.; Kaesz, H. D.; Khan, S. I.; Müller, H.-J. *Inorg. Chem.* **1990**, *29*, 1601.

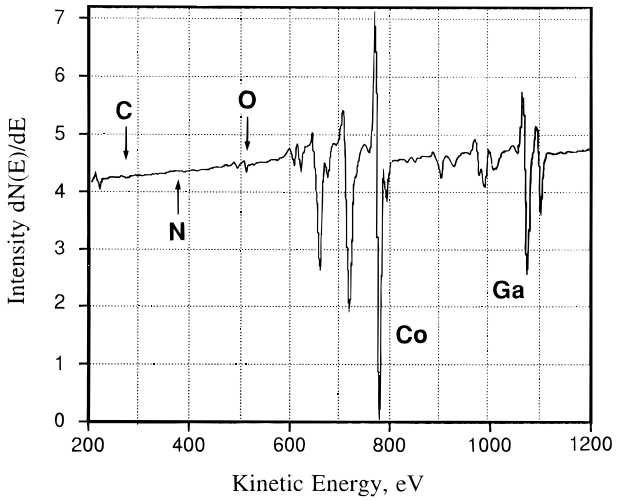

Figure 4. AES survey spectrum of the so far best CoGa film obtained from $(CO)_4CoGaEt_2(NMe_3)$ (**5a**; corresponds to Figure 3b).

Scheme 2

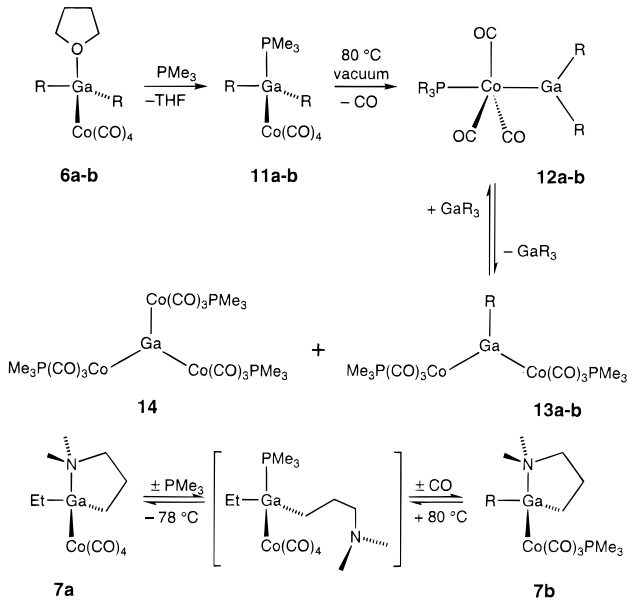

cobalt species (e.g., $Co_2(CO)_8$, $Co_3(CO)_{12}$) does not exist under our conditions. This explains why gallium rich films cannot be grown from the precursors examined in this study.

(a) Precursor Stability. For the precursor $(CO)_4Co-GaH_2(NMe_3)$ (**3**) the formation of thermally stable gallium species is impossible. According to the mechanism described above, digallane Ga_2H_6 or its trimethylamine adduct $H_3Ga-NMe_3$ may form either accompanying the sublimation of **3** and/or during the MOCVD process. But both gallium hydride compounds are very thermally labile[20] and will certainly decompose quantitatively at the conditions of the MOCVD experiments. For this reason CoGa films grown from **3** are never gallium deficient but sometimes gallium rich. This is explained by the thermal instability of the precursor **3** in the melt during sublimation, even at room temperature or below. **3** does not sublime without some decomposition, thus, some $H_3Ga-NMe_3$ and $[(CO)_4Co]_3Ga$ may form during sublimation of **3**. The analysis of the residue remaining after partial sublimation of **3** is indeed Co rich and shows the typical IR ν(CO) pattern of $[(CO)_4Co]_3Ga$.[4] Because $H_3Ga-NMe_3$ is much more volatile than $[(CO)_4Co]_3Ga$, the composition of the gas phase at the reactor inlet changes continuously during the MOCVD experiment. Therefore the obtained CoGa films exhibit a strong variation of the n(Co)/n(Ga) ratio with the depth of the film (Figure 3a). The Co/Ga layers which were grown at the early stages of the experiment are rather Ga rich with n(Co)/n(Ga) < 1. Which is caused by the relatively high amount of H_3GaNMe_3 compared to other volatile CoGa species. When most of the redistribution process has deceased and the composition in the bubbler has changed into $[(CO)_4Co]_3Ga$, then the grown layers become gallium deficient, n(Co)/n(Ga) > 1.

As was mentioned before, precursor **3** is a special case. All the other precursors do not show any comparable variation of the n(Co)/n(Ga) value with the depth (Figure 3b,c). Also, **1**–**2**, **4**–**8**, and **10** can be sublimed repeatedly without changing the composition of the sublimation residue or the sublimate. In solution **1**–**10** (except **3** of course) are perfectly stable against exchange of substituents at the gallium center. This is especially true for the intramolecularly base adduct derivatives. Bulky substituents and (intramolecular) Lewis base adduct formation generally stabilize dialkyl gallium transition metal compounds.[9]

The importance of a base adduct at the gallium center is nicely illustrated by the entries of Scheme 2. The compounds $(CO)_4Co-GaR_2(PR_3)$, (**11a,b**), which can be isolated in pure form, undergo an irreversible rearrangement upon heating in solution (closed system), which is accompanied by a subsequent fast alkyl exchange process.[10] This is much different for the intramolecularly base stabilized congeners.[9] The type of the Lewis base ligand also plays a role. While $(CO)_4Co-Ga(CH_3)_2(THF)$ (**4a**) is rather labile and transforms thermally into $[(CO)_4Co]_2Ga(CH_3)(THF)$, the closely related amine adduct $(CO)_4Co-Ga(CH_3)_2(NMe_3)$ (**4b**) is stable upon sublimation (50 °C, 10^{-3} Torr). The use of quinuclidine (NC_7H_{13}) as base ligand improves the stability against alkyl exchange even further. This is similar to the exceptional stability of $H_3Ga(NC_7H_{13})$[21] (sublimation without decomposition at 80 °C, 1 Pa) as compared to $H_3Ga-NMe_3$. The Ga–N donor bond is generally much stronger as compared to Ga–O and Ga–P Lewis donor–acceptor bonds.[22]

In summary, it can be ruled out that the variation of the metal ratio of the film with the substrate temperature is caused by premature decomposition upon volatilizing of the precursors **1**–**2**, **4**–**8**, and **10** examined in this study. This conclusion is also in full agreement with the representative mass balance given in Table 3.

(b) Gas Phase vs Surface Reactions. On the basis of a pressure between 0.1 and 10 Pa, the system is in the transition regime from viscous to free molecular flow.[23] The growth conditions used in this study are character-

(20) Greenwood, N. N.; Storr, A.; Wallbridge, M. G. H. *Inorg. Chem.* **1963**, *2*, 1036.

(21) Atwood, J. L.; Bott, S. G.; Elms, F. M.; Jones, C.; Raston, C. L. *Inorg. Chem.* **1991**, *30*, 3792.

(22) Elms, F. M.; Gardiner, M. G.; Koutsantonis, G. A.; Raston, C. L.; Atwood, J. L.; Robinson, K. D. *J. Organomet. Chem.* **1993**, 45.

(23) Ohring, M. *The Materials Science of Thin Films*; Academic Press: New York, 1992; Chapter 2, p 49.

ized by very high gas velocities of 2−3 m s^{-1}. It is therefore reasonable to assume that the precursor molecules are fairly "cold" when they arrive at the growth surface. The mechanism of the MOCVD process may thus be dominated by surface chemistry. Due to the lack of real-time in situ gas-phase analytical tools, it is however not absolutely clear to which extent homogeneous gas-phase reactions may also be important in controlling the decomposition chemistry of the precursors in addition to the heterogeneous surface reactions. In any case, the process described here is certainly far from equilibrium conditions.

The adsorption of $Ga(CH_3)_3$ (TMG) or $Ga(C_2H_5)_3$ (TEG) usually leads to the formation of R_2Ga species and adsorbed alkyl radicals at the growing surface.[24−28] For $Al(^iBu)_3$ (TIBA) it was shown that a selective β-hydride elimination reaction at the surface is important for the formation of isobuten and pure aluminum films.[29] Also, the disproportionation of $[(hfac)Cu^{I}L]$ precursors under MOCVD conditions to give pure Cu films and stable $(Hfac)_2Cu^{II}$ was shown to be a surface process.[30] These examples indicate that reaction patterns known from solution chemistry may be transferred conceptually to discuss surface reactions in MOCVD processes.

If homogeneous gas-phase reactions were dominant in determining the Ga loss by the formation of gallium alkyls, than one should expect that precursors which are stable against this process in solution (bulky substituents, intramolecular adduct formation) should give rather gallium deficient Co/Ga films at a given substrate temperature. However, this is not the case. The precursors bearing neopentyl ($CH_2{}^tBu$) or neosilyl (CH_2SiMe_3) substituents at the gallium center (**6a**,**b**) give very Co-rich films at low temperatures around 200−250 °C. The complexes **7a** and **8a** differ basically only by the alkyl substituents R at the Ga center but give the same temperature dependence of the metal ratio of the respective films. The compounds **5a** and **7a** differ only by the presence of a intramolecular chelate (**7a**), which blocks alkyl exchange significantly in solution. However, the intramolecularly adduct stabilized precursor **7a** gives much more Ga deficient films than its open chain congener **5a**. In addition, **7a** and **7b** exhibit different Co−Ga bond strengths due to trans phosphine substitution of **7b** but give virtually the same thin film results (Figure 2).

The important finding is that the *n*(Co)/*n*(Ga) value apparently follows the thermal stability of the gallium alkyls GaR_3 rather than the relative susceptibility of the precursors to undergo bimolecular ligand exchange reactions. This agrees also with the larger discrepancy of the different precursors in the temperature range between 200 and 300 °C as compared to temperatures above 300 °C.

It is interesting to compare these observations with the results of other studies focusing on the decomposition chemistry of gallium alkyls under the conditions of viscous flow, where homogeneous gas-phase reactions are dominant, rather than surface processes. Under steady-state conditions pure TMG diluted in an inert carrier gas starts to pyrolyse above 350 °C only.[31] The same is true for $Ga(CH_2{}^tBu)_3$,[32] $Ga(CH_2SiMe_3)$, and $R_2Ga[(CH_2)_3NMe_2]$.[33,34] The homogeneous decomposition of TEG however starts roughly 100 °C earlier, around 250 °C, because of the lower activation energy of the β-H elimination mechanism. According to Kaesz et al. a molar excess of at least 5−10 of TEG over $Cp(CO)_2Co$ is necessary to grow stoichiometric β-$Co_{0.50}Ga_{0.50}$ from those two sources under *atmospheric pressure* in the presence of hydrogen.[3] The need of a large gallium excess follows from the temperature dependence of the TEG pyrolysis under flow conditions, described above.[35,36]

The single source precursor **5a** represents the closest analogue to the combination TEG/$Cp(CO)_2Co$ so far. The temperature dependence of the Ga incorporation into the growing film however differs from the temperature dependence of the *vacuum* pyrolysis of pure TEG. In fact, *more* Ga is incorporated into the CoGa film than one would expect from the pyrolysis of TEG alone. Under our conditions, the very low efficiency (10−20%) of the vacuum pyrolysis of TEG alone does not change much between 200 and 300 °C. Thus, the molecular Co−Ga precursors, chemical derivatives of TEG, appear to be *activated* toward pyrolysis. This activation can be understood by regarding the stronger polarity of the Co−Ga bond compared to the Ga−C bonds, which allows a facile polar attack from surface sites to cleave the Co−Ga bond. The cleavage of the Co−Ga bond in solution is much faster that attack of the Ga−C bonds.[9,10]

In summary we thus suggest that the mechanism of the Ga loss is entirely a surface process. After splitting the Co−Ga bond of the precursor on the surface, a kinetic concurrence between the formation of easily desorbing trialkylgallium species and the fragmentation of the dialkylgallium species at the growing surface may take place. This process controls the metal stoichiometry (Scheme 3). The observed very strong dependence of the type of the alkyl group on the obtained metal ratio is a quite natural consequence of this mechanism. The importance of surface reactions is also indicated by the finding that the metal ratio of the films does not depend on the pressure (varied within the range 0.1−10 Pa).

Other recent examples of MOCVD processes which involve related ligand rearrangement processes at the growth surface include the following. The growth of copper films from (β-diketonato)$Cu^{I}L$ precursors (L = PR_3, $H_2C{=}CHSiMe_3$, etc.) involves the formation of (β-diketonato)$_2Cu^{II}$ in the course of a ligand migration at the copper surface.[30] Another type of rearrangement

(24) Donelly, V. M.; McCaulley, J. A. *Surf. Sci.* **1990**, *235*, L333.
(25) Yu, M. L.; Memmert, U.; Keuch, T. F. *Phys. Lett.* **1989**, *55*, 1011.
(26) Memmert, U.; Yu, M. L. *Appl. Phys. Lett.* **1990**, *56*, 1883..
(27) Creighton, R.; Lykke, K. R.; Shamamian, V. S.; Kay, B. D. *Appl. Phys. Lett* **1990**, *57*, 279.
(28) McCaulley, J. A.; McCrary, V. R.; Donnelly, V. M. *J. Phys. Chem.* **1989**, *93*, 1014.
(29) Bent, B. E.; Nuzzo, R. G.; Dubois, L. H. *J. Am. Chem. Soc.* **1989**, *111*, 1627.
(30) Kodas, T.; Hampden-Smith, M. in Kodas, T., Hampden-Smith, M., Eds; Verlag Chemie: Weinheim, 1994; p 264.
(31) Stringfellow, G. B. *Organometallic Vapor Phase Epitaxy*; Academic Press: San Diego, 1989.
(32) Almond, M. J.; Jenkins, C. E.; Rice, D. A. *J. Organomet. Chem.* **1993**, *443*, 137.
(33) Frese, V.; Regel, G. K.; Hardtdegen, H.; Bauers, A.; Balk, P.; Hostalek, M.; Lokai, M.; Pohl, L.; Mikilis, A. *J. Electron Mater.* **1990**, *19*, 305.
(34) Hostalek, M.; Pohl, L.; Brauers, A.; Balk, P.; Frese, V.; Hardtdegen, H.; Hövel, R.; Regl, G. K. *Thin Solid Films* **1989**, *174*, 1.
(35) Lee, P. W.; Omstead, T. R.; McKenna, D. R.; Jensen, K. F. *J. Cryst. Growth* **1988**, *93*, 134.
(36) Yoshida, M.; Watanabe, H.; Uesugi, F. *J. Electrochem. Soc* **1985**, *132*, 677.

Scheme 3

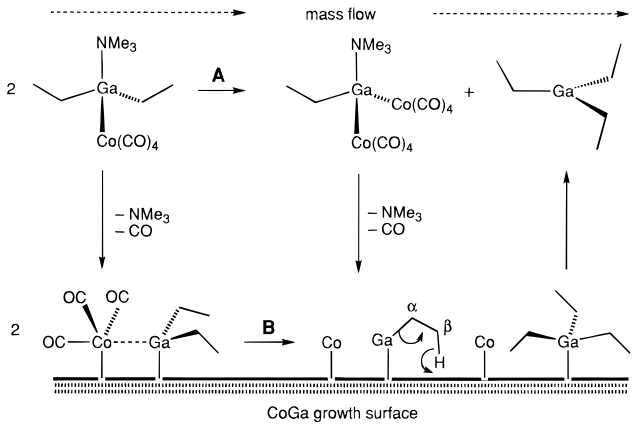

is important for the deposition of pure aluminum films from the precursor $(Me_3N)Al(H)_2(\mu^2\text{-}BH_4)$ reported by Spencer et al.[37] The transfer of the amine ligand from the aluminum to the boron center leads to the liberation of thermally stable $H_3B{-}NMe_3$. A similar reaction chemistry was observed during MOCVD of FeGa and FeAl thin films from $(\eta^5\text{-}C_5H_5)(CO)_2Fe{-}E[(CH_2)_3NMe_2]\text{-}(\eta^2\text{-}BH_4)$ (E = Al, Ga).[38,39] The alkylborane $H_2B[(CH_2)_3\text{-}NMe_3]$ was identified in the effluent. Last but not least we have recently described the deposition chemistry of ϵ-NiIn from $Cp(CO)Ni{-}In[(CH_2)_3NMe_2]_2$ in which CpIn is formed at low substrate temperatures by comparable mechanisms.[12]

To visualize the temperature dependency of the proposed alkyl exchange processes under MOCVD conditions in situ, the following experiment was conducted (Figure 6). A 1:1 gas-phase mixture of $(CO)_4Co{-}Ga(CH_3)_2(NMe_3)$ (**4b**) and $(CO)_4Co{-}Ga(C_2H_5)_2(NMe_3)$ (**5a**) was used to grow CoGa films (two different precursor vessels). The characteristic fragments $[GaMe_2^+]$ (m/z = 99); $[GaMeEt^+]$ (m/z = 115) and $[GaEt_2^+]$ (m/z = 129) were monitored by in situ mass spectroscopy. The fragments $[GaMe_2^+]$ and $[GaMeEt^+]$ constitute the base peaks of the electron impact mass spectra of both the used precursors **4b** and **5a** and the gallium alkyls $GaMe_3$ and $GaEt_3$, which are constituents of the effluent. Above 200 °C the precursors **4b** and **5a** are quantitatively pyrolyzed, e.g., no cobalt species passes through the hot tube (indicated by a significant drop of the characteristic peaks for $[(CO)_nCo^+]$). Also, by analyzing the contents of the cold trap the ratio n(Co)/n(Ga) was found to be less than 10^{-2} above 200 °C. Under these conditions, the intensities of the gallium fragments $[GaMe_2^+]$ (m/z = 99) and $[GaEt_2^+]$ (m/z = 127) are directly proportional to the amount of gallium alkyl which passes through without further pyrolysis. The mixed species $[GaMeEt^+]$ (m/z = 113) is an indication of alkyl exchange during the decomposition process. Figure 5 shows the normalized intensities of those fragments as a function of the oven temperature (the maximum intensities of the species at 200 °C were taken as the reference values I_0). At low temperatures up to 200 °C the signal intensities remain unchanged. Between 200 and 250 °C both precursors start to decompose. But while the $[GaEt_2^+]$ intensity drops continuously, the $[GaMe_2^+]$ intensity stays almost constant at a somewhat lower level until 350 °C and then drops sharply. As expected, the mixed species $[MeGaEt^+]$, which *must* arise from the discussed alkyl exchange mechanisms, was detected and exhibits its maximum intensity around 300 °C. It has to be pointed out, that the relative intensity of the mixed peak is only a function of the oven temperature and not of the pressure or the sublimation rate (by variation of the temperatures of the precursor reservoir).

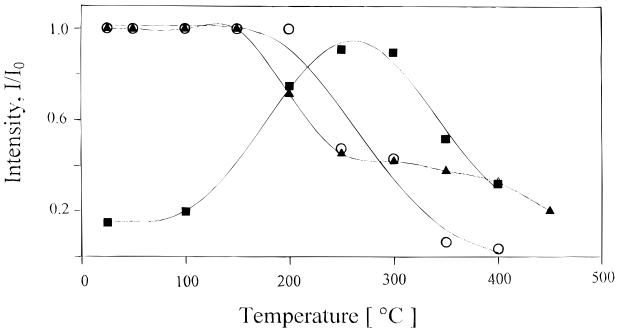

Figure 5. Relative intensities of the characteristic decomposition fragments (▲ = $[GaMe_2^+]$, ○ = $[GaEt_2^+]$, and ■ = $[MeGaEt^+]$) as a function of temperature using a 1:1 gas-phase mixture of the two precursors $(CO)_4CoGaMe_2(NMe_3)$ (**4b**) and $(CO)_4CoGaEt_2(NMe_3)$ (**5a**) (delivered from different and thermostated precursor vessels).

From mass spectroscopic studies[40] using the individual precursors **4b** and **5a** one can conclude, that the fragmentation of the Ga−N bond and/or one of the Co−CO bonds may be the first low-energy steps of the decomposition of the molecules. It is thus quite clear why the pyrolysis of both precursors starts very similarly at 200 °C. In the intermediate temperature range however, it might well be that the differences in the pyrolysis curves of **4b** and **5a** result from the different temperature dependence of the decomposition of the gallium alkyl fragments.

(c) Influence of the Co−Ga Bond Strength. It is very difficult to achieve a significant variation of the Co−Ga bond strength in structurally similar compounds of similar volatility. Only three precursors are available in this respect to compare with **5a,b**, **6a,b**, **7a**, and **8a,b**: $(Me_3P)(CO)_3Co{-}Ga[(CH_2)_3NMe_2]$(^{t}Bu) (**7b**), $(CO)_4\text{-}Co{-}GaCl_2(THF)$ (**1**), and $(Me_3P)(CO)_3Co{-}GaCl_2(NMe_3)$ (**2**). However, **1** and **2** contain halide substituents at the gallium center which makes these compounds rather different from the alkyl systems **4**−**10**. Trans phosphine substitution and/or halide substitution strengthens the Co−Ga bond, as is indicated by structural properties of the compounds (shorter bonds[10]) and the variation of their chemical reactivity 9−10. However under the conditions of electron impact mass spectroscopy, the relative intensity of peaks due to Co−Ga fragmentation relative to others with intact Co−Ga bond did not vary much.[40,41] Under our conditions the phosphine precursor **7b** showed the same temperature dependence of the Co/Ga ratio as its carbonyl congener **7a**. The halide precursors **1** and **2**, which are inert against the substituent-exchange reactions discussed

(37) Glass, J. A. J.; Kehr, S. S.; Spencer, J. T. *Chem. Mater.* **1992**, *4*, 530.
(38) Fischer, R. A.; Priermeier, T. *Organometallics* **1994**, *13*, 4306.
(39) Fischer, R. A.; T., P.; Scherer, W. *J. Organomet. Chem.* **1993**, *459*, 65.
(40) Kronseder, C.; Schindler, T.; Berg, C.; Fischer, R. A.; Niedner-schatteburg, G.; Bondybey, V. *J. Organomet. Chem* **1994**, *475*, 247.
(41) Kronseder, C. Diploma Thesis, Technische Universität München, 1993.

above, gave a much different temperature dependency of the metal ratio of the obtained films. A significant loss of Ga does only occur at the high temperature range (>350 °C). The mechanism of the Ga loss apparently involves the desorption of thermally stable GaCl species at high temperatures.[4] Films grown from **1**−**2** under vacuum at low temperatures contain a large amount of chlorine (up to 20 at. % by AES).

(d) Conclusive Remarks. Examining all the findings together, it may be concluded that a Co−Ga precursor related to **4**−**8**, which provides no possibility for alkyl exchange processes stressed above, will give stoichiometric CoGa films even at comparably low substrate temperatures. The GaR_2 units in the precursors **4**−**8** may present a problem, if very low substrate temperatures (<300 °C) are desired. To grow gallium-rich films, it will be necessary to synthesize precursors with a $CoGa_2$ stoichiometry. A precursor with such a $CoGa_2$ stoichiometry was reported by Kaesz et al. which indeed gave gallium rich films and proved this possibility. However in this compound the metals were linked by ancillary ligands involving σ(Ga−O) bonds rather than direct unsupported σ(Co−Ga) bonds. As a consequence of this, the obtained films were very oxygen rich and the decomposition temperature was rather high (∼550 °C).

For the binary alloys Fe/Ga and Cr/Ga we recently achieved our goals, the monoalkyl precursors $(CO)_nM$−GaEt(TMEDA) (M = Fe, n = 4; M = Cr, n = 5)[42] and the gallium-rich precursors $(CO)_4Fe\{Ga[(CH_2)_3NMe_2](^tBu)\}_2$.[43] The monoalkyl precursors $(CO)_nM$−GaEt(TMEDA) not only show much improved persistance of the M−Ga bond under the conditions of electron impact mass spectroscopy, they also do not show a temperature dependence of the metal ratio of the films. The compounds $(CO)_nM$−Ga(Et)(TMEDA) which still are structurally closely related to the CoGa family **1**−**10** are inert against alkyl exchange in solution. Apparently, the monoalkyl gallium fragment is short-lived enough at the growing surface and decomposes before any other more stable gallium species may have formed. This also agrees with the result, that using the Co_2Ga precursor **10**, exhibiting a monoalkylgallium fragment, the films were did not show a deviation from the preformed 2:1 ratio even at low deposition temperatures. As expected, the gallium rich precursors with direct M−Ga bonds, e.g., $(CO)_4Fe\{Ga[(CH_2)_3NMe_2](^tBu)\}_2$, give gallium-rich films at unprecedented low temperatures.[44] We are currently trying to extend these concepts to the Co/Ga precursor chemistry.

B. Purity of the Co/Ga Thin Films. The obtained thin films were routinely checked by AES (survey spectra and depth profiling with argon ion sputtering; see Figures 3 and 4). In selected cases, rather thick films were grown on the walls of the tube, which peeled off upon cooling and were collected. Subsequently combustion analysis were performed. A selection of representative results are compiled in Table 2 (Figure 3 and 4).

Results. The best thin-film quality was obtained using $(CO)_4Co-GaEt_2(NMe_3)$ (**5a**) as precursor compound. The AES survey spectra and depth profiles (Figure 3b and 4) show levels of C and O below 1 at. % throughout the bulk of the films. N was not detected by AES. Elemental analysis obtained from combustion and AAS of 50−60 mg samples of thin-film materials matches with the AES and EDX (metal content) values showing rather low contents of C, H, and O also (N was not detected). The C/H ratios were calculated to roughly 1. Also, chloride residues, which may result from impurities due to the precursor synthesis, were not detected. In the case of low temperatures and precursors with chelating alkyl substituents or alkyl substituents without β-hydrogen atoms (Me, $CH_2{}^tBu$, etc.), the obtained films were severely contaminated with hydrocarbon impurities, up to 15 at. % C (Figure 3c). The O and N contamination however did not significantly vary with the substrate temperature or the type of the precursor compound. The analysis of the condensable effluent proved the preferred formation of unsaturated hydrocarbons. The Lewis basic ligands, THF and NMe_3, were split off without further fragmentation.

Discussion. *(a) Carbon Impurities.* The use of carbonyl group (CO) containing precursors for MOCVD applications is a matter of controversial discussion. In principle, CO molecules can dissociatively chemisorb at metal surfaces, which ultimatively will lead to a more or less severe incorporation of carbidic carbon and oxygen atoms into the growing film. This *autocatalytic* mechanism is very important for the growth of "early" transition metals, e.g., Ti, Cr or Mo, from carbonyl compounds.[45] In the case of "late" transition metals (Co, Ni), this mechanism is much less important. Nothing is known to date about the chemisorption of CO on a CoGa single-crystalline surface. Our results may indicate that the residual carbon impurities are likely to be graphitic or hydrocarbons (C:H ∼1, by combustion analysis, see experimental part) but are not essentially carbidic. Firstly, high carbon contents never occur combined with high oxygen contents but are accompanied with rather high hydrogen levels (measured by combustion analysis; see C/H ratios of Table 2 and Figure 3). Also, the films grown from the hydride precursor **3** are essentially free of carbon and oxygen (Figure 3a). Precursors bearing alkyl substituents without β-hydrogen atoms or chelating aminoalkyl residues give high carbon levels up to 15−20 at. % at low temperatures (200−250 °C). But even at the high temperature range (>350 °C) the carbon impurities of 4−6 at. % are still quite severe. Also the asymmetric line profile of the carbon AES peak at 272 eV of the differentiated survey spectra is indicative for graphitic or hydrocarbon species. At least under our growth conditions, the alkyl substituents at the gallium atom are far more important in controlling the level of carbon impurities than the CO groups at the cobalt.

It is known from the GaAs semiconductor MOCVD chemistry that the mechanism of carbon incorporation involves surface bound Ga−C or As−C bonds.[46−48] The rate of carbon incorporation is much higher for $Ga-CH_3$

(42) Schulte, M. M.; Fischer, R. A.; Herdtweck, E. *Angew. Chem., Int. Ed. Engl.*, in press.
(43) Fischer, R. A.; Schulte, M. M.; Priermeier, T. *J. Organomet. Chem.* **1994**, *493*, 139.
(44) Fischer, R. A.; Miehr, A.; Schulte, M. *Adv. Mater.* **1995**, *7*, 58.
(45) Singmaster, K. A.; Houle, F. A.; Wilson, R. J. *J. Phys. Chem* **1990**, *94*, 6864.
(46) Kuech, T. F.; Veuhoff, E.; Kuan, T. S.; Deline, V.; Potemski, R. *J. Cryst. Growth* **1986**, *77*, 257.
(47) Kuech, T. F.; Veuhoff, E. *J. Cryst. Growth* **1984**, *68*, 148.
(48) Plass, C.; Heinecke, H.; Kayser, O.; Luth, H.; Balk, P. *J. Cryst. Growth* **1988**, *88*, 455.

than for $Ga-C_2H_5$ units under UHV conditions.[49] In our case reported here, the byproduct analysis indicate that the mechanism for the Ga−C bond cleavage involves β-elimination steps, since the ratio of unsaturated versus saturated hydrocarbon products is very high (>5−6). If β-elimination is blocked (e.g., precursors **6a,b**) higher carbon levels are the consequence. High-resolution mass spectroscopy of $(CO)_4Co-GaEt_2(NMe_3)$ (**5a**) using a Fourier transform ion cyclotron mass spectrometer showed the characteristic and correlated fragments $[(CO)_nCoGaEt^+]$ and $[(CO)_nCoGaH^+]$, which support the possibility of *homogeneous* β-elimination upon excitation of the molecule (UHV conditions). The chelating alkylamine ligands of **7** and **8** are somewhat a problem in this respect (Figure 3c). While it is clear from the byproduct analysis, that unsaturated amines such as $H_2C{=}CHCHNMe_2$ dominate the fragment pattern, the amount of saturated amines is quite substantial (15−20 mol %), indicating less selective radical reactions. This may be understood by regarding the blocking of the Ga center by the (chelating) alkylamine donor. The C levels are significantly larger compared with the ethyl precursor **5a**. Interestingly, nitrogen could not be detected by AES in these cases. The condensable effluent however contained a few volume percent NMe_3 and $MeNEt_2$. The electron mass spectra of the compounds $(CO)_4Co-Ga[(CH_2)_3NR^1_2](R)$ typically show the fragment $[H_2C{=}NR^1_2{}^+]$ as the base peak.[9−11,39,43] This may indicate the possibility of a C−C bond cleavage within the carbon chain of the propylamine group under MOCVD conditions and may thus account for the not detected N content in the respective films. In this context it is interesting to note that the C levels of aluminum films grown from $R_2Al[(CH_2)_3NMe_2]$ are 2 orders of magnitude higher than the C levels of aluminum films grown from TIBA.[50]

(b) Oxygen Impurities. A residual oxygen content of 1−4 at. % remained rather constant throughout the bulk of the samples (AES depth profiling, Figure 3 and 4). These traces are most likely caused by the leaking rate of the MOCVD apparatus as well as being imported during the general manipulation of the precursor compound itself. The precursors are rather moisture sensitive which could result in a small contamination with oxygen containing products. Those products are also volatile and decompose during MOCVD to give gallium oxide (Ga_2O_3). However, a rigorous exclusion of oxygen and moisture was not possible due to lack of appropriate instrumentation (for example, a glovebox connected to the CVD apparatus to allow clean transfer of precursors and coated substrates). The analysis of the background gases by mass spectrometry showed partial pressures of $\sim10^{-7}$ Torr for H_2O and $\sim10^{-8}$ Torr for O_2 at a total base pressure of $\sim10^{-5}$ Torr at the reaction zone (mostly hydrocarbons and CO). From these numbers a maximum limit of 1−10 at. % of oxygen incorporation may be estimated.[51] Related precursors, which are much less sensitive toward hydrolysis than **1**−**10**, but contain the same $(CO)_4Co$ unit show systematically lower O levels throughout the bulk of the films. This is true for example for $(CO)_4Co-In[(CH_2)_3NMe_2]_2$[52] and $(CO)_4Co-As[\eta^2-(^tBuN-CH_2CH_2-N^tBu)]$[53] (both less than 0.5 at. %, by AES).

After the film growth is completed, the surface of the films is always covered with high hydrocarbon and oxygen impurities, which is probably caused by the condensation of nonfragmented precursor molecules and hydrolysis of those upon exposition of the films to the air by opening the reactor after the experiment was finished (Figure 4c). Those impurities are removed by a 1−2 min of initial sputter cleaning of the surface (Figure 3b).

(c) Nitrogen and Phosphorous Impurities. Within the accuracy of the AES method, N incorporation was not detected. Nonchelating amine ligands are split off without any further fragmentation. This is not surprising, because the N−C bonds are rather stable and do not cleave (without catalysis) below 500 °C. In case of the chelating alkyl amine ligands some NMe_3 or $MeNEt_2$ and 1-ethylazetidine (∼5 mol %) were detected in the effluent, which may account for the not detectable N content besides significant carbon levels, as discussed above already. Also, when using precursor **7b,** P traces were not detected by AES.

(d) Other Impurities. Besides the above-mentioned species, which are interesting with respect to the precursor design, other trace impurities, which may arise from the precursor synthesis (Cl, Li, Si, Zn, Fe, etc., introduced by the used reagents and starting materials) are far less important in determining the bulk properties of the deposited alloy (metallic conductivity, crystallinity). If necessary, those contaminants can certainly be avoided by employing electronic grade starting materials and optimized synthesis conditions. Cl contaminations were not detected by AES. Other trace impurities were not checked.

(e) Metallic Conductivity. The best values of the specific resistivity for the *n*(Co)/*n*(Ga) films close to the 1:1 stoichiometry were measured to 120−150 $\mu\Omega$ cm. Depending on the impurities and the size of the crystallites, relatively high specific resistivities of 500−1000 $\mu\Omega$ cm were measured. A stoichiometric $Co_{0.50}Ga_{0.50}$ alloy exhibits a bulk resistivity of 100−120 $\mu\Omega$ cm.[54] The best values of MOCVD grown CoGa films from two independent precursors were also close to 120 $\mu\Omega$ cm.[3] The quality of the best CoGa films grown from our precursors is thus in good agreement with those standards.

C. Crystallinity, Phase Identity, and Thin-Film Reactions. Structural Characterization. The binary Co/Ga phase diagram shows five regions between 25 and 800 °C, which differ in composition and structure: α-$Co_{1-y}Ga_y$ ($y \leq 12$ at. %; α-CoGa, single phased; solid solution of Ga in Co with the structure of α-Co.), α-CoGa + β-CoGa (∼12−30% Ga, two phase region), β-CoGa (∼30−60% Ga, cubic, B2 type, single phased), β-CoGa + $CoGa_3$ (∼60−75% Ga, two phase region) and $CoGa_3$ (>75% Ga, single phased).[55−57] The $Co_{0.50}Ga_{0.50}$

(49) Miller, J. E.; Eckerdt, J. G. *Chem. Mater.* **1994**, *6*, 343.
(50) Kamp, M.; König, F.; Mörsch, G.; Lüth, H. *J. Cryst. Growth* **1992**, *120*, 124.
(51) Murarka, S. P. *Metallization*; Butterworth-Heinemann: Stoneham, 1993; p 111.
(52) Fischer, R. A.; Herdtweck, E.; Priermeier, T. *Inorg. Chem.* **1994**, *33*, 934.
(53) Herrmann, W. A.; Fischer, R. A.; Klingan, F. R.; Miehr, A. *Appl. Phys. Lett.*, **1995**, *67*, 822.
(54) Yamaguchi, Y.; Kiewitt, D. A.; Aoki, T.; Brittain, J. O. *J. Appl. Phys.* **1968**, *39*, 231.
(55) Bither, T. A.; Cloud, W. H. *Appl. Phys.* ***1965.***, *36*,, 1501.
(56) Schubert, K.; Meissner, H.-G.; Raman, A.; Rossteuscher, W. *Naturwissenschaften* **1964**, *51*, 287.
(57) Meissner, H.-G.; Schubert, K. *Z. Metallkde.* **1965**, *56*, 523.

phase forms peritectically at 1483 K upon melting the two metals together at 1500 K, annealing over several days at 1173 K and slow cooling (100 K/day) to room temperature.[58,59] The range of existence of the β-CoGa phase is quite large and spans from 34.4 to 57.8 mol % of gallium content. As a consequence of the cubic defect structure of the alloy the lattice parameter varies from 287.5 pm at 34.4% Ga over 288.3(1) pm at 50% Ga to 285.3(5) pm at 57.6% Ga.[59] The enthalpy of formation of the CoGa alloy amounts to −10 kcal/mol.[60]

All Co/Ga films obtained on chemically inert substrates (borosilicate glass, fused silica or sapphire) proved to be polycrystalline β-CoGa. The measured *d* spacings are in full agreement with reference data.[59] A typical film (no. 12 of Table 2b) with an analytical composition close to 1:1 exhibited the dominant 110 reflection at a value of $2\theta = 44.64(4)°$, which corresponds to a lattice constant of 287.88(1) pm (Table 3). Given the above mentioned variation of the lattice constant with the gallium ratio,[59] a gallium content of only 40% would be calculated. This does not agree with the AAS values of the particular films. Various Co/Ga thin film samples with metal ratios of 1.05(±0.5) gave lattice constants around 288(±0.3) pm which is acceptably close to the value of 288.3(1) pm for pure polycrystalline $Co_{0.50}Ga_{0.50}$. The small deviations may also be a consequence of the residual C and O contaminations of the films. The experimental density (pycnometrically) of the obtained CoGa material ranges around 7.9(5) g cm^{-3}, which is reasonably close to the density obtained from the lattice parameters of 8.9 g cm^{-3} and reference values of 8.7(±0.5) g cm^{-3}.[59] Therefore it may be concluded that the content of amorphous materials of the films is quite low.

Thin-Film Reactions. The chemical stability of elemental Co and CoGa films of various composition with respect to GaAs has been thoroughly investigated.[61−64] Gallium-deficient CoGa films tend to react with the GaAs surface to give other phases, $CoGa_3$ and CoAs, etc., besides β-CoGa. Slightly gallium-rich CoGa films which are perfectly lattice matched to GaAs are stable up to 600 °C. The best of our stoichiometric $Co_{0.50}Ga_{0.50}$ films grown from $(CO)_4Co{-}GaEt_2(NMe_3)$ on GaAs showed some preferred orientation in the 110 direction and were stable up to 300 °C (Figure 6a). Slightly gallium-deficient films grown from **4b** at 350 °C exhibit significant amounts of other phases, e.g., $CoGa_3$, and CoAs, as one would expect (Figure 6b). CoGa films grown on silicon at 350 °C also showed some reactivity toward the silicon surface. The corresponding XRD patterns prove the presence of other phases, α-CoGa, Co_2Si, $CoGa_3$, etc. (Figure 6c).

We have so far not grown epitaxial CoGa films on GaAs(100), which should be possible and had actually been achieved previously by molecular beam epitaxy (MBE)[2,64] and MOCVD of CoGa from separate sources.[3] This is presumably mostly due to our somewhat nonperfect treatment of the GaAs substrates and growth conditions. To achieve epitaxial growth, usually a gallium-terminated GaAs surface is prepared prior to CoGa deposition.[3,62]

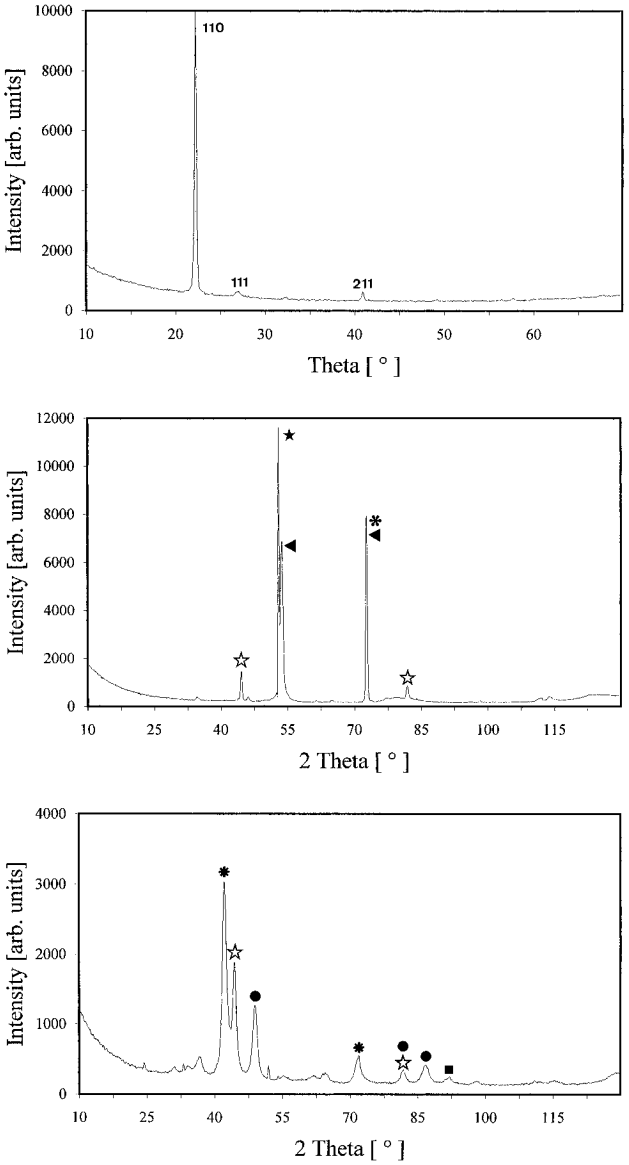

Figure 6. X-ray diffraction patterns: (a, top) single-phase β-CoGa on GaAs(100) grown from **5a** at 280 °C, 1 Pa (6 h, 1 μm; ∼0.2 μm h^{-1}). (b, middle) Multiphase CoGa film grown from **5a** at 400 °C, 1 Pa on GaAs(100) (3 h, 1 μm; ∼0.3 μm h^{-1}): ★ β-Co_2As (211); ▲ CoAs (130), (222); ☆ β-CoGa (110), (211); ∗ $CoGa_3$ (224). (c, bottom) Multiphase CoGa film grown from **5a** at 400 °C, 1 Pa on silicon(100) (3 h, 1 μm; ∼0.3 μm h^{-1}) after subsequent annealing at 450 °C for 2 h: ✱ α-CoGa (111), (220); ☆ β-CoGa (110), (211); ● Co_2Si (311), (521 or 041); (023 or 241); ■ CoSi (322 or 410).

Conclusion

The successful growth of comparably pure polycrystalline binary Co_1Ga_{1-x} ($0 \le x \le 0.65$) alloy thin films from a series of dialkylgallium tetracarbonyl cobalt complexes with a 1:1 metal ratio was demonstrated. In terms of deposition conditions and thin-film quality, the best single-source precursor to deposit stoichiometric $Co_{0.50}Ga_{0.50}$ at the moment appears to be $(CO)_4Co{-}$

(58) Köster, W.; Horn, E. *Z. Metallkde.* **1952**, *43*, 333.
(59) Wunsch, K. M.; Wachtel, E. *Z. Metallkde.* **1982**, *73*, 311.
(60) Feschotte, P.; Eggimann, P. *J. Less-Common Met.* **1974**, *63*, 15.
(61) Shiau, F.-Y.; Zuo, Y.; Lin, J.-C.; Zheng, X.-Y.; Chang, Y. A. *Z. Metallkde.* **1989**, *80*, 544.
(62) Zhu, J. G.; Carter, C. B.; Palmstrøm, C. J.; Garrison, K. C. *Appl. Phys. Lett.* **1989**, *55*, 39.
(63) Shiau, F. Y.; Chang, Y. A.; Chen, L. J. *J. Electron. Mater.* **1988**, *17*, 433.
(64) Kuo, T. C.; Kang, T. W.; Wang, K. L. *J. Cryst. Growth* **1991**, *111*, 996.

$GaEt_2(NMe_3)$. The study of the decomposition chemistry of **3**−**10** under isothermal vacuum conditions without carrier gases showed that, at a given substrate temperature between 200 and 400 °C, the metal ratio of the CoGa films is controlled by the alkyl substituents at the gallium center. The decomposition mechanism of the precursors involves alkyl exchange or migration reactions at the growth surface, which lead to relatively stable trialkylgallium species. Precursors, for which such reactions are disfavored compared to further gallium alkyl fragmentation (Ga−C bond splitting) or are even impossible (Ga−H) give perfectly stoichiometric CoGa films, even at rather low temperatures. The purity of the best films compares to other MOCVD grown CoGa materials. The observed thin film reactivity above 350 °C agrees with the nonepitaxial nature of the films and their stoichiometry. To achieve the deposition of gallium-enriched and thus more stable CoGa films on GaAs from related cobalt carbonyl precursors, it will be necessary to synthesize molecular precursors with a $CoGa_2$ stoichiometry in which the metals are directly linked together without ancillary ligands. For the related Fe/Ga system we have recently shown that such a compound can be synthesized, $(CO)_4Fe\{Ga[(CH_2)_3NMe_2](^tBu)\}_2$, and serves as a suitable precursor to deposit very pure $FeGa_{2-x}$ ($x \leq 0.1$) films by similar techniques.[44] As a consequence of our findings described above, we are currently working on the synthesis of related cobalt compounds which may be suitable as a precursors to deposit the desired gallium rich β-$Co_{0.45}Ga_{0.55}$ films, which are perfectly lattice matched to GaAs(100).

Acknowledgment. This work was supported by the Deutsche Forschungsgemeinschaft (Grant No. Fi 502/2-2 and 2-4), the Fonds der Chemischen Industrie, the Friedrich Schiedel Foundation, and the Leonhardt Lorenz Foundation. The assistance of Prof. F. Baumgärtner and Dr. G. Henkelmann (Institute of Radiochemistry, Technical University at Muinich and Prof. E. Born, Dr. Th. Metzger (Institute of Mineralogy Technical University at Muinich) with surface analysis and structural characterization of the thin film is gratefully acknowledged.

CM9504044